ELSEVIER

Nuclear Instruments and Methods in Physics Research A 459 (2001) 543–551

NUCLEAR INSTRUMENTS & METHODS IN PHYSICS RESEARCH Section A

www.elsevier.nl/locate/nima

X-ray-induced radiation damage in CsI, Gadox, Y_2O_2S and Y_2O_3 thin films

A.S. Tremsin*, J.F. Pearson, A.P. Nichols, A. Owens[1], A.N. Brunton, G.W. Fraser

X-ray Astronomy Group, Space Research Centre, Department of Physics and Astronomy, University of Leicester, Leicester LE1 7RH, UK

Received 18 April 2000; received in revised form 15 August 2000; accepted 31 August 2000

Abstract

The stability of CsI, CsI(Tl), Gd_2O_2S(Tb), Gd_2O_2S(Eu), Y_2O_2S(Eu) and Y_2O_3(Eu) thin films under bombardment by 9–18 keV X-rays is described. Both external photocurrent and scintillation light yield were measured as functions of accumulated dose at radiation fluxes of 10^6–10^7 photons s^{-1} mm^{-2} on Beamline 2.2 of the Daresbury Synchrotron Radiation Source (SRS). All of the samples studied showed changes of several percent (both reductions *and* increases) in photocurrent and scintillation light yield of several percent for accumulated doses of up to 5×10^{11} photons mm^{-2}. No significant dependence of the film response on the angle of X-ray incidence was observed for angles up to 45° from the normal. It was found that the accumulated dose is not the only parameter determining the degradation of photoconverter performance; the flux rate has also to be taken into account. Scanning Electron Microscope studies of the irradiated samples did not reveal any significant surface modification.

Keywords: Photocathodes; Scintillators; Radiation damage

1. Introduction

The radiation hardness of thin film scintillators such as CsI and GdO_2S_2 (Gadox) is of concern for several detector applications involving high X-ray fluxes, e.g. synchrotron-based protein crystallography (PX) [1] and non-destructive evaluation [2]. In the case of scintillator-coupled Charge Coupled Devices (CCDs) used in PX, a change in detector sensitivity of only a few percent in an intensively illuminated area will affect the determination of relative Bragg peak intensities and hence may compromise the accuracy of a crystal structure determination. In other fields, such as Cherenkov light imaging [3] and e-beam production using laser-driven sources [4] radiation damage in CsI and similar photocathodes is equally important. Radiation damage in photoconverters in general has therefore been the subject of a number of recent studies [5–8]; UV-induced radiation damage in alkali halide photocathodes has been studied in particular detail [9–11]. Previous reports from our laboratory [12,13] have described the decay (and

* Corresponding author: Present address: Experimental Astrophysics Group, Space Sciences Laboratory, University of California at Berkeley, Berkeley CA 94720, USA. Tel.: +1-510-642-4554; fax: +1-510-643-9729.

E-mail address: ast@ssl.berkeley.edu (A.S. Tremsin).

[1] Now at: Astrophysics Division, ESA ESTEC, Postbus 299, 2200 AG Noordwijk, The Netherlands.

0168-9002/01/$ - see front matter
PII: S0168-9002(00)01059-7

recovery when bombardment is interrupted) of the external photoyield from CsI, CsI(Tl) and KBr under exposure to 0.1–3 keV X-rays at grazing incidence.

In the present paper we describe a systematic experimental study of the changes induced by X-rays in the energy band 9–18 keV in both the photocurrent (Section 3.1) and scintillation light yield (Section 3.2) of several widely used photoconverters: CsI, CsI(Tl), Gadox(Tb), Gadox(Eu), Y_2O_2S(Eu) and Y_2O_3(Eu). The photoconverters were in the form of thin films. The 9–18 keV energy band is that commonly used in synchrotron-based PX experiments. We considered the influence of X-ray intensity, as well as that of accumulated dose, on the processes taking place in the photoconverters (Section 3.3). Finally, the results of a Scanning Electron Microscope (SEM) study of the irradiated films are presented in Section 3.4.

2. Measurements

Measurements were made on Beamline 2.2 of the Daresbury Synchrotron Radiation Source (SRS) (UK). Each experiment consisted of the simultaneous monitoring of the replacement current and the light yield from a sample illuminated with monochromatic radiation of energies 9, 12, 15 or 18 keV. The nominal beam profile at the sample was $1 \times 4\,mm^2$.

2.1. Sample preparation

The CsI and CsI(Tl) photocathodes were thermally evaporated in vacuum onto $28 \times 12\,mm^2$ stainless-steel substrates at Leicester. The coating rate was 20–40 Å s^{-1}; during deposition the substrates were maintained at a nominal temperature of 100°C. A value of 14 000 Å was chosen based on previous experience with CsI photocathodes deposited on microchannel plate (MCP) X-ray detectors. All samples of a given material were prepared simultaneously in order to eliminate any possible differences in the photocathode performance due to the differences between particular deposition runs. After coating, the samples were stored in a dry nitrogen atmosphere in a desiccator until required at the synchrotron.

The Gadox(Tb) (Gd_2O_2S(Tb) or P43) samples were prepared by Applied Scintillation Technologies Ltd. (formerly Levy Hill Laboratories) [14] with a coating weight of $10\,mg\,cm^{-2}$. The Gadox(Eu), Y_2O_2S(Eu) and Y_2O_3(Eu) scintillators of the same coating weight were provided by Photonic Science Ltd. [15]. The same stainless-steel substrates were used for all samples.

Since the external X-ray photocurrent from insulators is dominated by low-energy ($\sim$eV) secondaries originating in a surface layer a few hundred Angstroms thick, all our thin films are "asymptotically thick" with respect to measurements of photocurrent. Our rare earth phosphor layer thicknesses are typical of those used in PX applications while the vacuum-evaporated CsI and CsI(Tl) layers, viewed as scintillators, are rather thin ($\sim$0.6 versus $\sim 10\,mg/cm^2$ in a working detector).

2.2. Beamline and calibration chamber

The sample substrates were attached, four at a time, to demountable angled plates fixed on a mounting arm. The angled plates defined the angles of X-ray incidence to the samples: 90° (normal incidence), 75°, 60° or 45° relative to the photocathode surface. Using a linear drive with a 50 mm travel, we could illuminate any of the four samples without breaking vacuum.

The calibration vacuum chamber had a 200 μm thick Al entrance window with a calculated transmission shown in Table 1. The transmission at 6 keV was very low (only 0.24%) and considering the degree of harmonic contamination from the monochromator at 6 keV, we chose our lowest operating energy to be 9 keV.

The light yield from the samples was monitored by a Hamamatsu H5784-04 photomultiplier (PMT), which was mounted next to the sapphire window of the calibration chamber and shielded from ambient light by a light cover. The replacement photocurrent into the sample substrates was measured by a Keithley electrometer.

2.3. Beam intensity calibration

Beam intensity was monitored by an air-filled ion chamber positioned before the calibration

Table 1
Calculated transmission of the chamber entrance window.

Beam energy (keV)	6	9	12	15	18
Window transmission (%)	0.24	15.8	45.8	67.3	79.7

Table 2
Linear absorption coefficient μ for 1 bar air [16]

E (keV)	9	12	15	18
$\mu(10^{-3}\,\mathrm{cm}^{-1})$	9.14	3.54	1.69	0.93

Table 3
Estimated beam intensities

E (keV)	9	12	15	18
N'_{ph} (10^7 photons $\mathrm{s}^{-1}\,\mathrm{mm}^{-2}$)	7.2	7.4	2	0.47

chamber and intended primarily to calibrate the decay of the X-ray flux, rather than, as below, to measure the absolute beam intensity. The ion chamber current represents the number of electron–ion pairs produced in the gas per second (N_{ion}). The X-ray energy absorbed in the ion chamber per second, I_{abs}, can be calculated as follows:

$$I_{\mathrm{abs}} = I_{\mathrm{beam}}(1 - \exp(-\mu L)) = N_{\mathrm{ph}}E(1 - \exp(-\mu L)) \quad (1)$$

where L is the ion chamber length (~ 2 cm), N_{ph} is the beam flux in photons per second and E is the X-ray energy. We assumed that production of each ion–electron pair required an energy $W = 25$ eV, allowing Eq. (1) to be rewritten as follows:

$$WN_{\mathrm{ion}} = N_{\mathrm{ph}}E(1 - \exp(-\mu L)). \quad (2)$$

The actual photon flux at the sample N'_{ph} can be calculated from the following equation:

$$N'_{\mathrm{ph}} = CN_{\mathrm{ph}}\exp(-\mu L) \quad (3)$$

where C is the transmission of the chamber entrance window (Table 1). Substituting N_{ph} from Eq. (2), the desired N'_{ph} at the sample is given by

$$N'_{\mathrm{ph}} = C[WN_{\mathrm{ion}}]/[E(\exp(\mu L) - 1)]. \quad (4)$$

Values for the linear absorption coefficient μ at the relevant energies were taken from Ref. [16] and are shown in Table 2.

Table 3 indicates typical values of the beam intensity per unit illuminated area at normal incidence.

2.4. Measurement sequences

Samples were irradiated for standard periods of 60 or 120 min and the relative variation of photocurrent and light yield measured as functions of X-ray dose. Absolute values of photocathode quantum efficiency and of the light yield of scintillators have been reported elsewhere [2,17,18]. A fresh sample was used for each test. To check repeatability, a number of repeat measurements on different samples of some types were performed. In order to sample rapid initial changes, the replacement current and PMT signal were recorded in 1 s bins for the first 5 min, 5 s bins for the following 15 minutes, and 10 s bins for the remaining 40 or 100 min. The study of photoconverter recovery [12,13] after an interruption of the X-ray irradiation was not possible on Beamline 2.2. The investigation of recovery phenomena requires that the flux be the same before and after the gap in irradiation. In the absence of a sample shutter, closure of the beamline stop, placed before the monochromator, was the only method of interrupting the flux on the sample. After opening the stop, the flux measured by the ion chamber was unstable for at least 30 s, presumably due to thermal stabilisation effects in the monochromator.

3. Results and discussion

3.1. Photocurrent variation

Figs. 1–6 illustrate the relative variation with X-ray dose of the photocurrent from CsI, CsI(Tl), Gadox(Tb), Gadox(Eu), Y_2O_2S(Eu) and

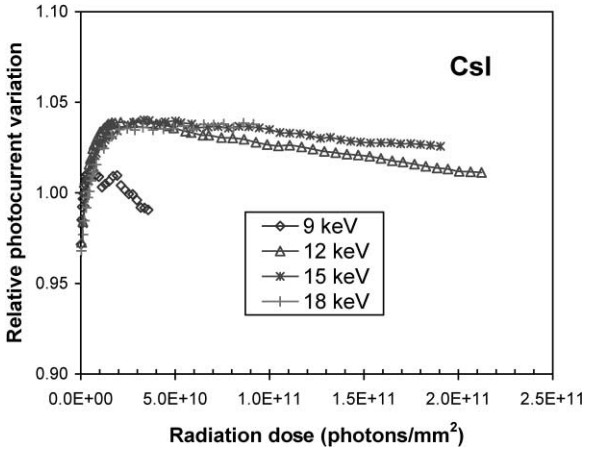

Fig. 1. Normalised photocurrent from CsI thin films as a function of accumulated X-ray dose for different X-ray energies; normal incidence.

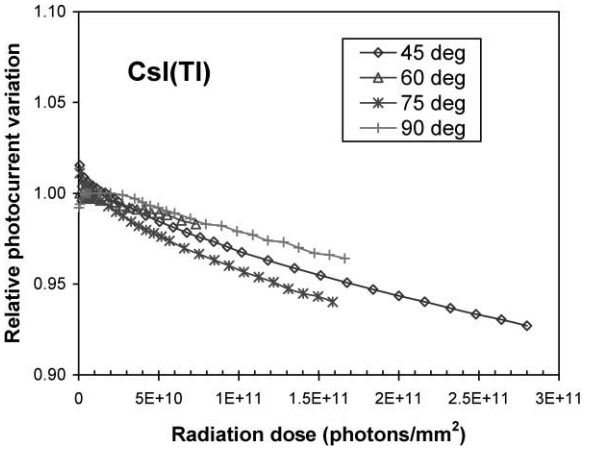

Fig. 3. Normalised photocurrent from CsI(Tl) thin films as a function of accumulated 9 keV X-ray dose for different photon incidence angles (relative to the photocathode surface).

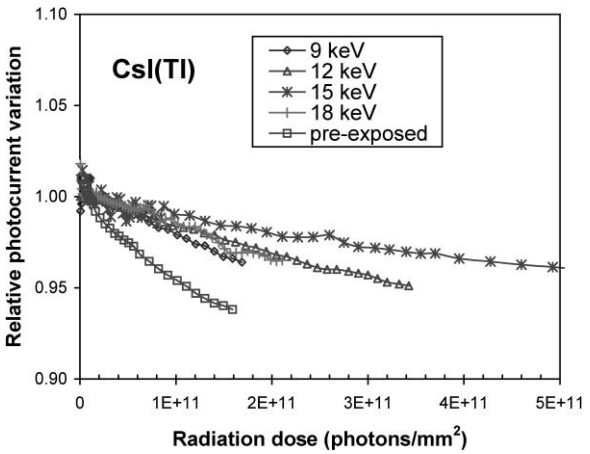

Fig. 2. As Fig. 1, except CsI(Tl) photocathodes.

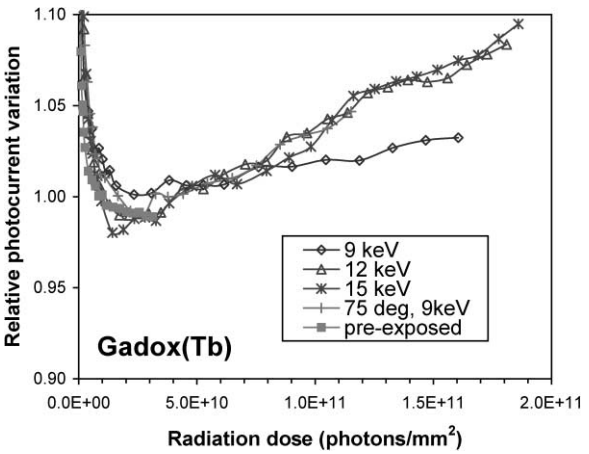

Fig. 4. As Fig. 1, except Gadox(Tb) photocathodes; normal incidence unless otherwise stated.

Y_2O_3(Eu), respectively, measured for our four chosen beam energies and at specified angles of incidence.

The pure CsI photocathodes (Fig. 1) showed a relatively fast increase in the quantum efficiency at the beginning of each measurement cycle, followed by a gradual decay of the photocurrent. CsI(Tl), by contrast, showed no initial increase of the photocurrent, which decayed monotonically (Fig. 2) at approximately the same rate as that observed for pure CsI. We also investigated the photocurrent decay of CsI(Tl) samples irradiated at 9 keV at different incidence angles, as shown in Fig. 3. X-rays with larger incidence angles are absorbed closer to the photocathode surface. One might therefore expect to observe faster degradation rates for larger incidence angles relative to the normal if the processes contributing to radiation damage had an important surface component. Fig. 3 offers no support for this hypothesis; the rate of decay is not simply correlated with angle of incidence.

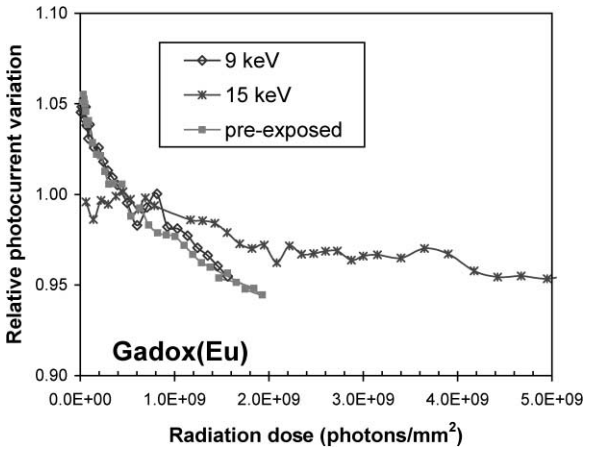

Fig. 5. As Fig. 1, except Gadox(Eu) photocathodes.

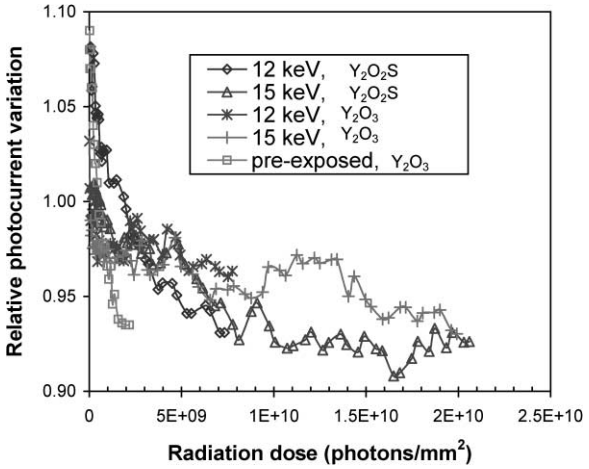

Fig. 6. As Fig. 1, except Y_2O_2S(Eu) and Y_2O_3(Eu) thin films.

The photocurrent–dose curves for Gadox(Tb) shown in Fig. 4 have a different form from those of either CsI or CsI(Tl). A fast initial decrease in photocurrent to about 90% of its initial value at doses of 1.25×10^{10} photons mm^{-2} is followed by a gradual recovery of the photoelectron emission efficiency. This behaviour is not present in the limited Gadox(Eu) data of Fig. 5. Both Y_2O_2S(Eu) and Y_2O_3(Eu) samples (Fig. 6) had a sharp 10–15% photocurrent decrease at doses of $\sim 2.5 \times 10^9$ photons mm^{-2} followed by a very slow photocurrent decay. The data of Figs. 4–6 are noisy compared to those for pure and doped CsI because the absolute values of the photocurrent from Gadox, Y_2O_2S and Y_2O_3 samples were relatively small.

3.2. Variation in light yield

Both CsI and CsI(Tl) scintillator layers exhibited a two-component increase in light yield with accumulated dose, for all energies investigated: a fast increase up to doses of $\sim 10^{10}$ photons mm^{-2}, followed by a relatively slow increase in the light output of several percent per 2×10^{11} photons mm^{-2} (see Figs. 7–10). As with photocurrent, we did not observe a simple dependence of the light output on the angle of incidence.

For terbium-doped Gadox scintillators (Fig. 11), we observed an essentially monotonic increase of the photoyield of the film with radiation dose (an increase of about 6% per 10^{11} photons mm^{-2}). For Gadox(Eu), we noted a small decrease in scintillation light with dose (Fig. 12), although further studies are necessary for this material to extend the accumulated dose. Both Y_2O_2S(Eu) and Y_2O_3(Eu) scintillators (Fig. 13) appeared to be relatively stable under X-ray exposure; their light yields increased only by 2–3% after 2×10^{10} photons mm^{-2} irradiation.

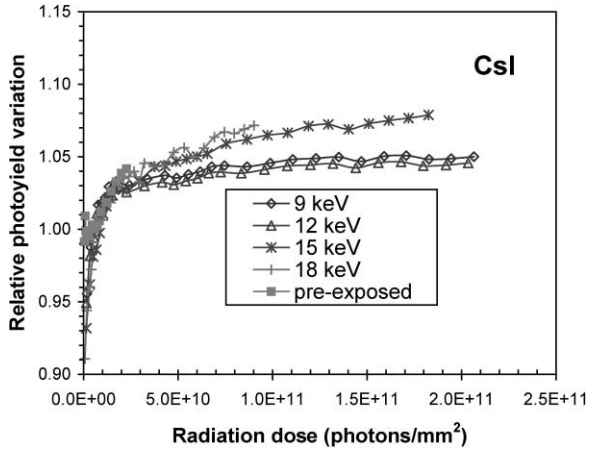

Fig. 7. Normalised light yield from CsI thin films as a function of accumulated X-ray dose for different X-ray energies; normal incidence.

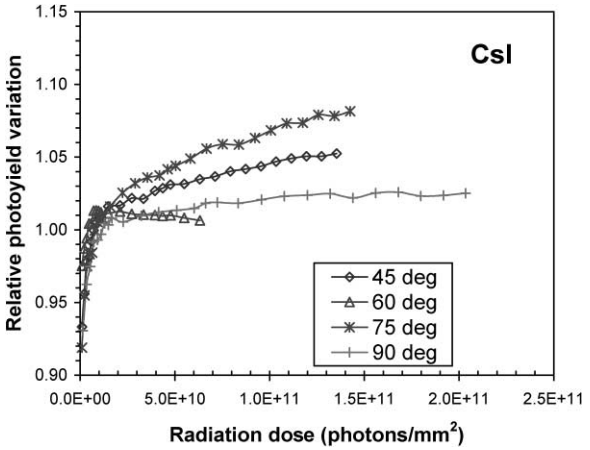

Fig. 8. Normalised light yield from CsI thin films as a function of accumulated 9 keV X-ray dose for different photon incidence angles (relative to the photocathode surface).

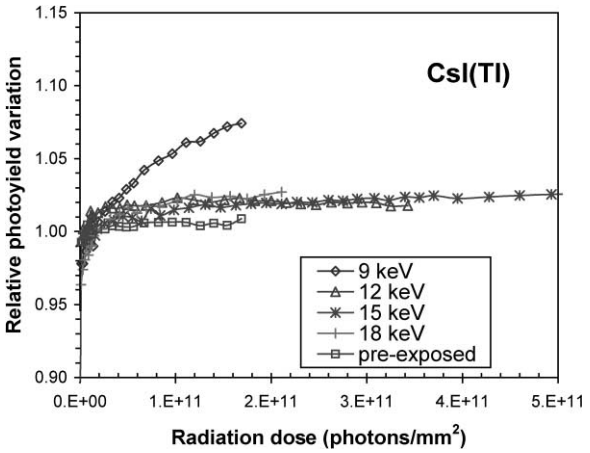

Fig. 9. As Fig. 7, except CsI(Tl) thin scintillator films.

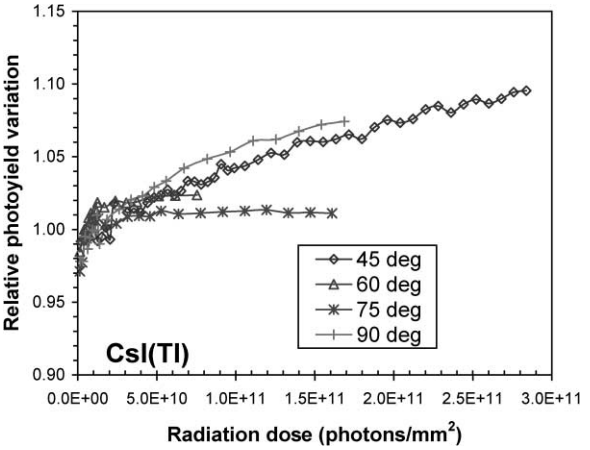

Fig. 10. As Fig. 8, except CsI(Tl) thin scintillator films.

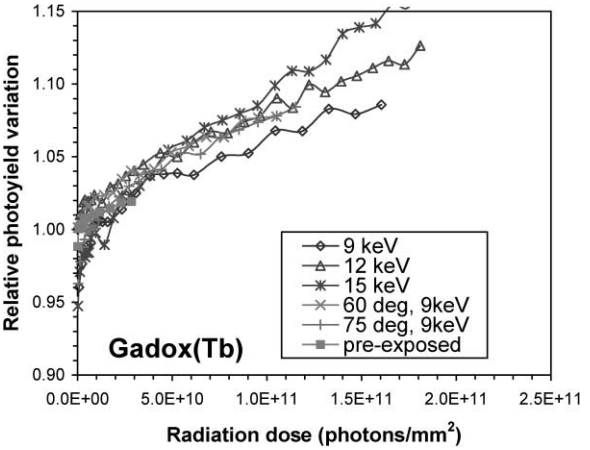

Fig. 11. Normalised light yield from Gadox(Tb) thin films as a function of accumulated X-ray radiation dose for different energies; normal incidence if not otherwise stated.

3.3. The dependence of radiation damage on flux rate

In this section, we describe our investigations of the importance of the absolute value of radiation flux. Some of the samples were exposed to synchrotron white beam (full spectra) radiation on SRS Beamline 8.4 for several seconds, prior to study of their response on Beamline 2.2. We estimate that this "pre-exposure" involved a photon dose of 10^{13}–10^{14} photons mm^{-2} for a continuum spectrum between 1 and 25 keV. Exposure of a standard microscope slide to the same dose resulted in a strong colouration of the exposed glass area.

Measurements of the response of pre-exposed samples for an X-ray energy of 9 keV are shown in Figs. 2–13. Despite the large energy dose suffered by the pre-irradiated samples, the subsequent photocurrent and photoyield variation with radiation dose is similar to that of the fresh samples, except for CsI(Tl). The photocurrent of pre-irradiated CsI(Tl) (Fig. 2) dropped by 6.2% at a dose of 1.25×10^{11} photons mm^{-2}. The corresponding drop for a fresh sample was 3.4%. The light yield of pre-irradiated CsI(Tl) (Fig. 9) did not exhibit any

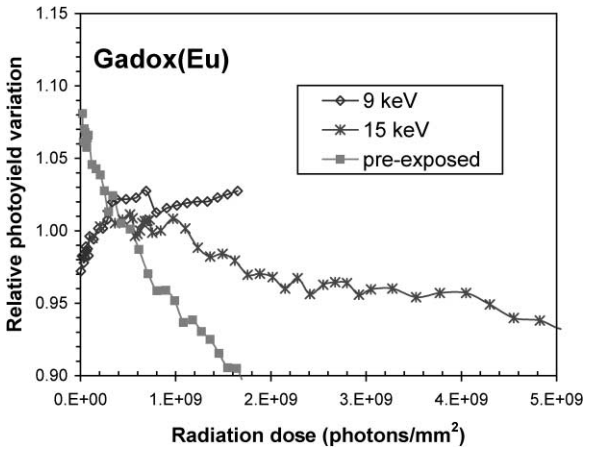

Fig. 12. As Fig. 7, except Gadox(Eu) thin scintillator films.

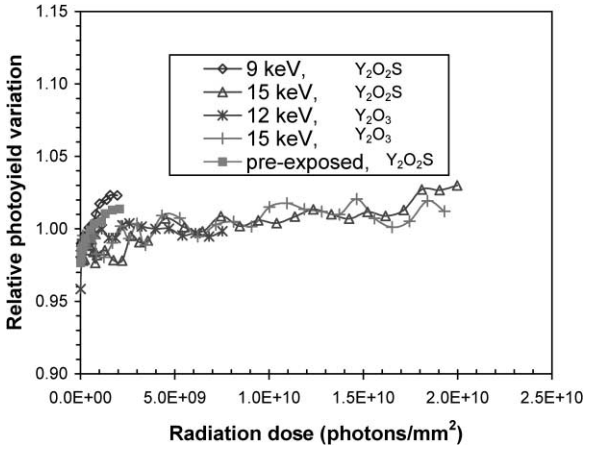

Fig. 13. As Fig. 7, except Y_2O_2S(Eu) and Y_2O_3(Eu) thin scintillator films.

increase with dose, unlike the fresh film. Due to the absolute flux calibration restraints we could not study in detail the decrease in the absolute values of the photocurrent and light yield after white beam exposure. However, the accuracy of our measurements is sufficient to rule out any order of magnitude decrease in either photocurrent or light yield.

3.4. SEM studies

We used a Scanning Electron Microscope (Medical Sciences, University of Leicester) to study possible surface changes after the samples were irradiated. The images of fresh CsI and CsI(Tl) samples (Figs. 14a and 15a) were recorded for comparison with those of films exposed at 9 keV (about 10^{12} photons mm^{-2}) and also to white beam illumination, as described in Section 3.3. No evidence for surface modification in either material was observed, in contrast to the results of previous studies (see Ref. [12] and references therein). Both irradiated and fresh samples had been stored in a desiccator for several days before the SEM images were taken. Ideally, SEM images should have been acquired immediately following X-ray exposure, given that the surface metallisation of CsI films [12,19,20] following X-ray bombardment may conceivably be reversible on air exposure.

4. Conclusions

The photocurrent and photoyield from six commonly used thin film photoconverters change by several percent for accumulated 9–18 keV X-ray doses of up to 5×10^{11} photons mm^{-2}. The form of the decay curve varies from material to material and between photocurrent and scintillation light yield for a given material. Our data set should prove useful, for example, in the design of detectors for applications such as synchrotron protein crystallography; the remarkable (linear) increase in light yield with dose for terbium-doped Gadox (Fig. 11) does not appear to have been previously discussed in the literature.

At a more fundamental level, a photoconverter model is required which simultaneously accounts for the variation in photocurrent (including the recoveries reported in other studies [12,13]) and the variation in light yield in a given material at a given X-ray energy, with the rate of X-ray absorption as a significant parameter (at least for CsI(Tl)). Previously, a yield-dose function of the form

$$\chi(D) = a_1 + a_2 \exp(-c_2 D) + a_3 \exp(-c_3 D) \qquad (4)$$

has been used to account for the electron-induced decrease in UV quantum efficiency of CsI [21] and the soft X-ray-induced reduction in photocurrent from CsI and KBr [13]. Such a representation is clearly inadequate for the present Gadox(Tb)

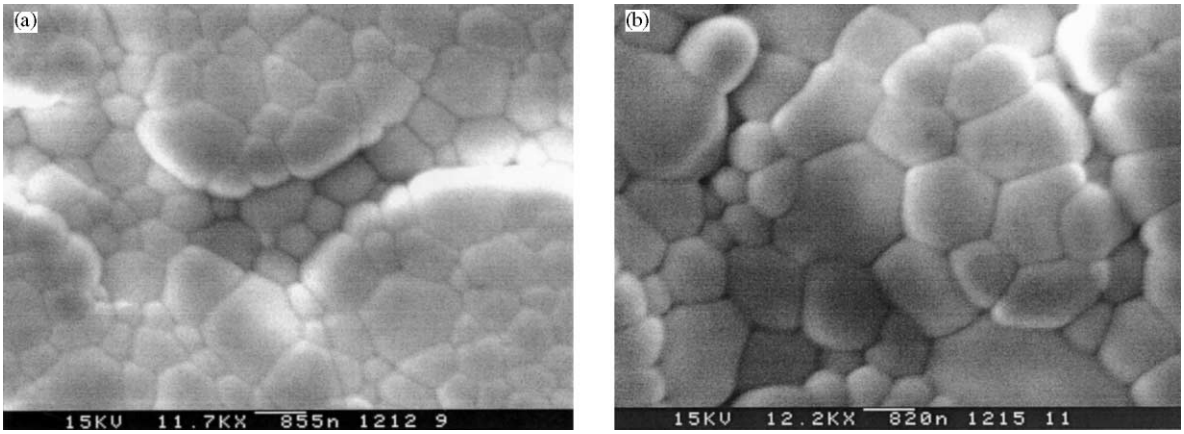

Fig. 14. Scanning electron microscope (SEM) images of fresh (a) and irradiated (b) CsI thin film samples. The irradiated sample was exposed to 10^{12} photons mm^{-2} at flux rate of 7×10^{7} photons s^{-1} mm^{-2} and then to $\sim10^{14}$ photons at flux rate of 10^{13} photons s^{-1} mm^{-2}. Scale indicated by tick marks.

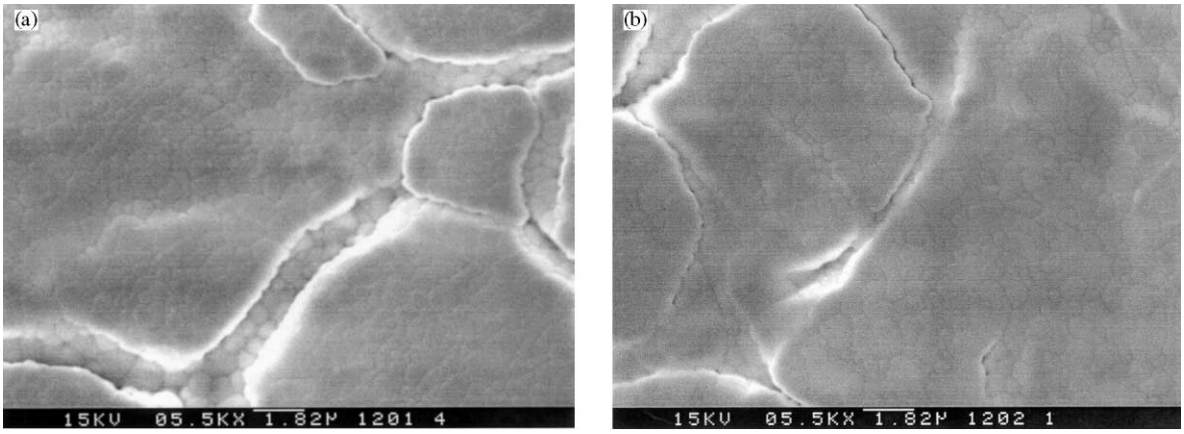

Fig. 15. Scanning electron microscope images of fresh (a) and irradiated (b) CsI(Tl) thin film samples. The irradiated sample was exposed to 10^{12} photons mm^{-2} at flux rate of 7×10^{7} photons s^{-1} mm^{-2} and then to $\sim10^{14}$ photons at flux rate of 10^{13} photons s^{-1} mm^{-2}. Scale indicated by tick marks.

photocurrent data and for most of our scintillation light measurements.

The construction of a physical model for the kinetics of X-ray radiation damage in a photoconverter such as CsI must take into account such bombardment rate-dependent processes as F- and H-type colour centre formation, the diffusion and recombination of these centres in the bulk of the layer, the formation of alkali metal colloids as well as ion and neutral emission from the surface. One of us [13] has adapted the models of Jain and Lidiard [22] and Soppe [23] to produce a system of stiff ordinary differential equations representing the creation and decay of colour centres; the decay in photocurrent with X-ray dose may then be calculated from the reciprocal addition of the electron escape length in undamaged material and the electron mean free path due to F-centres. This work will be described in a later contribution; unfortunately, values for the required rate constants and

cross-sections are unknown for all the photoconverters described in this paper so an ab initio calculation of decay curves is not presently possible.

Acknowledgements

The authors wish to thank Applied Scintillation Technologies and Photonic Science for providing the rare earth phosphors and Jason Page for his assistance with the in house coatings and measurements. APN acknowledges the receipt of a PPARC Ph.D. studentship. This work was made possible by CLRC beamtime award 27/290.

References

[1] E.M. Westbrook, Proc. SPIE 3774 (1999) 2.
[2] V.V. Nagarkar, S.V. Tipnis, T.K. Gupta, S.R. Miller et al., IEEE Trans. Nucl. Sci. NS-46 (1999) 232.
[3] F. Piuz, Nucl. Instr. and Meth. A 371 (1996) 96.
[4] E. Chevallay, L. Durand, S. Hutchins, G. Suberlucq et al., Nucl. Instr. and Meth. A 340 (1994) 146.
[5] K. Kazui, A. Watanabe, S. Osone, B.G. Cheon et al., Nucl. Instr. and Meth. A 394 (1997) 46.
[6] M.A.H. Chowdhury, A. Holmes-Siedle, A.K. McKemey, S.J. Watts et al., Nucl. Instr. and Meth. A 413 (1998) 471.
[7] R.-Y. Zhu, Nucl. Instr. and Meth. A 413 (1998) 297.
[8] J. Brose, G. Dahlinger, K.R. Schubert, Nucl. Instr. and Meth. A 417 (1998) 311.
[9] C. Lu, Z. Cheng, D.R. Marlow, K.T. McDonald et al., Nucl. Instr. and Meth. A 371 (1996) 155.
[10] J. Vavra, A. Breskin, A. Buzulutskov, R. Chechik, E. Shefer, Nucl. Instr. and Meth. A 387 (1997) 154.
[11] A.S. Tremsin, O.H.W. Siegmund, Nucl. Instr. and Meth. A 442 (2000) 337.
[12] G.W. Fraser, M.T. Pain, J.F. Pearson, J.E. Lees, C. Binns, P.S. Shaw, J.R. Fleischman, Proc. SPIE 1548 (1991) 132.
[13] A.P. Nichols, University of Leicester Ph.D. Thesis 1996.
[14] Applied Scintillation Technologies Ltd., 8 Roydonbury Industrial Estate, Harlow CM19 5BZ, UK.
[15] Photonic Science Ltd., Millham, Mountfield, Robertsbridge, East Sussex TN32 5LA, UK.
[16] M.V. Zombeck, High energy astrophysics handbook, Smithsonian Astrophysical Observatory, Special Report 386, 1980.
[17] R.M. Rideout, J.F. Pearson, G.W. Fraser, J.E. Lees, A.N. Brunton, N.P. Bannister, A.T. Kenter, R.P. Kraft, Proc. SPIE 3445 (1998) 384.
[18] S.E. Pearce, J.E. Lees, J.F. Pearson, G.W. Fraser, A.N. Brunton, K.A. Flanagan, A.T. Kenter, M. Barbera, V. Dhanak, A. Robinson, D. Teehan, Proc. SPIE 2518 (1995) 322.
[19] R.M. Wilson, W.E. Pendleton, R.T. Williams, Radiat Effects Defects Solids 128 (1994) 79.
[20] R.M. Wilson, R.K.R. Thoma, W.E. Pendleton, R.T. Williams, Nucl. Instr. and Meth. B 91 (1994) 12.
[21] D.F. Anderson, S. Kwan, V. Peskov, B. Hoeneisen, Nucl. Instr. and Meth. A 323 (1992) 626.
[22] U. Jain, A.B. Lidiard, Phil. Mag 35 (1977) 245.
[23] W.J. Soppe, J. Phys, Condens. Matter 5 (1993) 3519.